

NASA Technical Paper 3554

1N-37
56-56-6
p. 33

Analysis of Stress Concentration at Holes in Components Made of 2195 Aluminum-Lithium

ORIGINAL CONTAINS
COLOR ILLUSTRATIONS

2

R. Ahmed

(NASA-TP-3554) ANALYSIS OF STRESS
CONCENTRATION AT HOLES IN
COMPONENTS MADE OF 2195
ALUMINUM-LITHIUM (NASA, Marshall
Space Flight Center) 33 p

N95-30613

Unclas

H1/39 0056566

May 1995



Analysis of Stress Concentration at Holes in Components Made of 2195 Aluminum-Lithium

R. Ahmed
Marshall Space Flight Center • MSFC, Alabama

TABLE OF CONTENTS

| | Page |
|----------------------------|------|
| INTRODUCTION | 1 |
| BACKGROUND | 1 |
| ANALYSIS METHODOLOGY | 2 |
| RESULTS | 2 |
| DISCUSSION..... | 3 |
| CONCLUSIONS | 3 |
| REFERENCES..... | 26 |

LIST OF ILLUSTRATIONS

| Figure | Title | Page |
|--------|--|------|
| 1. | Geometry used in plate with hole analysis..... | 6 |
| 2. | MSFC ANSYS model used in plate with hole analysis..... | 7 |
| 3. | 2195 Al-Li and 2219 Al stress-strain curves..... | 8 |
| 4. | 2195 Al-Li and 2219 Al stress-strain curves..... | 9 |
| 5. | Maximum hole strain versus far-field stress, 2195 Al-Li, $F_{tu} = 78$ ksi, $F_{ty} = 73$ ksi, ultimate strain = 0.04 | 10 |
| 6. | Maximum hole stress versus far-field stress, 2195 Al-Li, $F_{tu} = 78$ ksi, $F_{ty} = 73$ ksi, ultimate strain = 0.04 | 11 |
| 7. | Maximum hole strain versus far-field stress, 2195 Al-Li, $F_{tu} = 82$ ksi, $F_{ty} = 77$ ksi, ultimate strain = 0.04 | 12 |
| 8. | Maximum hole stress versus far-field stress, 2195 Al-Li, $F_{tu} = 82$ ksi, $F_{ty} = 77$ ksi, ultimate strain = 0.04 | 13 |
| 9. | Maximum hole strain versus far-field stress, 2195 Al-Li, $F_{tu} = 78$ ksi, $F_{ty} = 73$ ksi, ultimate strain = 0.06 | 14 |
| 10. | Maximum hole stress versus far-field stress, 2195 Al-Li, $F_{tu} = 78$ ksi, $F_{ty} = 73$ ksi, ultimate strain = 0.06 | 15 |
| 11. | Maximum hole strain versus far-field stress, 2195 Al-Li, $F_{tu} = 78$ ksi, $F_{ty} = 75$ ksi, ultimate strain = 0.06 | 16 |
| 12. | Maximum hole stress versus far-field stress, 2195 Al-Li, $F_{tu} = 78$ ksi, $F_{ty} = 75$ ksi, ultimate strain = 0.06 | 17 |
| 13. | Maximum hole strain versus far-field stress, 2195 Al-Li, $F_{tu} = 78$ ksi, $F_{ty} = 77$ ksi, ultimate strain = 0.06 | 18 |
| 14. | Maximum hole stress versus far-field stress, 2195 Al-Li, $F_{tu} = 78$ ksi, $F_{ty} = 77$ ksi, ultimate strain = 0.06 | 19 |
| 15. | Maximum hole strain versus far-field stress, 2195 Al-Li, $F_{tu} = 80$ ksi, $F_{ty} = 79$ ksi, ultimate strain = 0.06 | 20 |
| 16. | Maximum hole stress versus far-field stress, 2195 Al-Li, $F_{tu} = 80$ ksi, $F_{ty} = 79$ ksi, ultimate strain = 0.06 | 21 |

LIST OF ILLUSTRATIONS (Continued)

| Figure | Title | Page |
|--------|---|------|
| 17. | Maximum hole strain versus far-field stress, 2195 Al-Li, $F_{tu} = 78$ ksi, $F_{ty} = 77$ ksi, ultimate strain = 0.08 | 22 |
| 18. | Maximum hole stress versus far-field stress, 2195 Al-Li, $F_{tu} = 78$ ksi, $F_{ty} = 77$ ksi, ultimate strain = 0.08 | 23 |
| 19. | Plot of von Mises stress for 2195 plate with hole, $F_{tu} = 78$ ksi, $F_{ty} = 73$ ksi, ultimate strain = 4 percent, far-field stress = 60 ksi..... | 24 |
| 20. | Plot of axial strain for 2195 plate with hole, $F_{tu} = 78$ ksi, $F_{ty} = 73$ ksi, ultimate strain = 4 percent, far-field stress = 60 ksi..... | 25 |

LIST OF TABLES

| Table | Title | Page |
|-------|---|------|
| 1. | Hole stresses and strains versus far-field stress for various 2195 Al-Li materials..... | 4 |
| 2. | Hole stresses and strains versus far-field stress for various 2195 Al-Li materials..... | 5 |

TECHNICAL PAPER

ANALYSIS OF STRESS CONCENTRATION AT HOLES IN COMPONENTS MADE OF 2195 ALUMINUM-LITHIUM

INTRODUCTION

To enable the space shuttle to reach the space station high-inclination orbits with adequate payload, an effort was made in the early 1990's to reduce the weight of the space shuttle external tank (ET) and/or the solid rocket boosters (SRB's). This culminated in the design of the super lightweight ET (SLWT ET), whose goal was to reduce ET weight by at least 8,000 lb. To accomplish this, NASA and Martin Marietta (the prime contractor for the ET) proposed replacing most of the 2219 aluminum used in the current ET with the lighter, stiffer, and stronger 2195 aluminum-lithium (Al-Li) alloy. Design changes were also proposed to take advantage of the increased strength and modulus of the new alloy over 2219.

Since the 2195 alloy initially used in the SLWT ET program had a small (less than 5 ksi) difference between the yield and ultimate strengths when compared to 2219 (about 13 ksi difference), ET engineers became concerned over how this material would behave in regions of stress concentration. This paper deals with the effect of stress concentration at holes on the material behavior of 2195 and the concerns this raised over vehicle robustness.

BACKGROUND

In the design of a space vehicle such as the ET, particular attention must be paid to areas of stress concentration. These include holes, weld lands, inserts, fillets, welds, and other areas that tend to create load and stiffness gradients. Such locations have local areas of much higher stress than would be found or expected in larger, more uniform sections. For instance, in a linear elastic analysis the maximum stresses around a hole under uniform tension are three times the nominal far-field stress, and local plastic yielding will occur wherever the hole stress is greater than or equal to the yield stress. Loads of this magnitude tend to be redistributed to regions farther away from the hole as a result of the plastic behavior of the material, thus relieving the stress and preventing failure as long as the stress and strain of the highest loaded position in the body remains below the ultimate value. In order to accomplish this stress redistribution effectively, the material must have a sufficient area under the plastic region of the stress-strain curve; this area is governed both by the material's ultimate strain capability and the difference between the ultimate and yield strengths (henceforth referred to as the yield-ultimate delta).

During preliminary design of the SLWT ET, the 2195 Al-Li alloy showed a lower yield-ultimate delta than the 2219 alloy used previously. As a result, ET designers and analysts became concerned that 2195 might not redistribute the load around stress concentrations adequately enough to prevent failure at far-field stresses below yield. To examine this behavior more closely, elastic-plastic structural analyses of typical stress concentration configurations were made. These included areas around holes and a typical weld land geometry found in the liquid oxygen (lox) tank. The effort concentrated primarily on analysis of holes, since these have the highest stress concentration factors. Corresponding analysis was performed for holes using the 2219 alloy for comparison. 2219 had a yield-ultimate delta of 13 ksi with a maximum strain of 10 percent, whereas the corresponding worst-case values for 2195 were 5 ksi and 4 percent, respectively. Since the weld land analyses showed only a very slight plastic strain, this paper concerns itself only with the hole analyses.

ANALYSIS METHODOLOGY

The analysis was performed via a quarter-symmetric, nonlinear plastic finite element model of a 3.75-in wide, 0.3-in thick, 12-in long test specimen with a 0.375-in diameter hole in the center (fig. 1). The finite element model is shown in figure 2. The model was generated using the PATRAN preprocessing code, with the analysis being performed by the ANSYS finite element solver. The model was run with several different stress-strain curves for comparison (figs. 3 and 4). The material properties and stress-strain data used for these analyses were taken from preliminary data supplied by both NASA and Martin Marietta.

By taking advantage of symmetry planes, only one-fourth of the specimen needed to be modeled. This minimized the model size. The model consisted of 1,896 four-noded quad ANSYS SHELL43 elements and 2,009 nodes with a concentrated mesh around the hole to provide greater accuracy near the area of stress concentration. Appropriate symmetry boundary conditions were applied, and fixed displacements corresponding to the applied forces were applied on the loaded edge in order to ease convergence. The model was sufficiently long to avoid a significant reduction of the boundary forces resulting from yielding of the material. (Using applied forces at the boundary created substantial convergence problems and significantly increased run time). In all cases run, the maximum longitudinal stress and strain occurred at the hole locations whose tangents are parallel to the specimen longitudinal direction.

Investigations were made of the effects of changing various parameters, such as yield strength, ultimate strength, and ultimate strain. Of primary interest was determining the highest axial stress and strain at the hole perimeter. The axial stress and axial strain were then plotted as a function of far-field axial stress for each combination of yield strength, ultimate strength, and ultimate strain. From these data, the far-field stress required to induce failure at the hole could be determined for each material combination.

Stresses, strains, and displacements were graphically displayed via color contour plots using ANSYS' built-in postprocessing capability. This produced attractive, fine resolution color plots that clearly showed stress, strain and displacement values, gradients, and trends.

RESULTS

The tabulations of maximum axial hole stresses and strains versus far-field tensile stress are shown in tables 1 and 2. The corresponding graphs of these quantities are shown in figures 5 through 18. Sample plots showing a typical stress distribution from one of the analysis runs are shown in figures 19 and 20.

DISCUSSION

The following phenomena were observed from the analysis data:

- (1) The far-field stress required to induce failure at the hole does not appreciably change as the yield strength approaches the ultimate strength while holding the ultimate strain constant.
- (2) Increasing the failure strain capability of the material increases the far-field stress required to induce failure at the hole. However, the material response curve (stress versus strain) at the hole edge does not appreciably change.
- (3) Decreasing the ultimate strain capability significantly decreases the far-field load-carrying capability of the structure.

An important point of consideration in these analyses and in the corresponding tests is comparing the failure stress at the hole with the net section-failure stress (caused by the absence of material at the hole). If the two values are very close to each other, not much can be said about whether or not stress concentrations have a serious impact on structural performance. To mitigate this effect, the model size must be tailored such that the ratio of hole diameter to specimen width is sufficiently low.

The far-field stress capability of the 4-percent ultimate strain Al-Li material was by far the lowest of all the materials examined—only 60 ksi was required to cause failure at the hole for the material that would be used in the SLWT ET liquid hydrogen tank (with 73-ksi yield and 78-ksi ultimate strength). This was a serious reduction in strength capability over the nominal 78-ksi ultimate strength and was actually lower than the 64 ksi required to cause failure in an identical geometry made from 2219 aluminum alloy.

On the other hand, the far-field stress capability of the 8-percent ultimate strain Al-Li indicated a significant increase in overall stress capability. A 70-ksi far-field stress was required to cause failure at the hole. This was exactly equivalent to the stress required for net section failure, indicating that hole stress concentrations had no significant effect on tension failure for this material and geometry.

CONCLUSIONS

The analyses showed that hole stress concentrations were a serious issue of concern for the 2195 Al-Li material with less than 4-percent ultimate strain capability, exhibiting a significant reduction in load carrying capability due to reaching ultimate stress and strain at the highest stressed position on the hole. However, yield-ultimate deltas ranging from 1 to 5 ksi did not result in a significant variance in the far-field stress capability of specimens of a given ultimate strength and ultimate strain. Thus, the most important factor influencing the far-field strength of the material was the ultimate strain. The analyses showed that, for the specimen geometry tested, 2195 material with a 4-percent ultimate strain must be loaded at a far-field tensile stress below 60 ksi to prevent failure at the hole edge. Regions of the SLWT ET or any vehicle using current versions of 2195 AL-Li that contain holes and/or inserts must be designed to keep the stresses below these reduced values to ensure the structural integrity of the vehicle.

Table 1. Hole stresses and strains versus far-field stress for various 2195 Al-Li materials.

SLWT ET Stress Concentration Analyses, 3.75-in Wide Plates With Holes

2195 Al-Li, $F_{tu} = 78$ ksi, $F_{ty} = 73$ ksi, $\epsilon_{psult} = 0.06$

| Far-Field Stress (ksi) | Max Strain at Hole | Max Stress at Hole (ksi) | Net Section Stress (ksi) |
|------------------------|--------------------|--------------------------|--------------------------|
| 24.3 | 0.006636 | 73.00 | 27.00 |
| 45 | 0.0186 | 74.12 | 50.00 |
| 50 | 0.0227 | 74.50 | 55.56 |
| 55 | 0.0281 | 75.00 | 61.11 |
| 60 | 0.0416 | 76.28 | 66.67 |
| 65 | 0.053 | 77.35 | 72.22 |
| 67 | 0.06 | 78.00 | 74.44 |

2195 Al-Li, $F_{tu} = 78$ ksi, $F_{ty} = 75$ ksi, $\epsilon_{psult} = 0.06$

| Far-Field Stress (ksi) | Max Strain at Hole | Max Stress at Hole (ksi) | Net Section Stress (ksi) |
|------------------------|--------------------|--------------------------|--------------------------|
| 25 | 0.006818 | 75.00 | 27.78 |
| 45 | 0.0182 | 75.64 | 50.00 |
| 50 | 0.0223 | 75.88 | 55.56 |
| 55 | 0.0269 | 76.14 | 61.11 |
| 60 | 0.0397 | 76.86 | 66.67 |
| 65 | 0.0518 | 77.55 | 72.22 |
| 67 | 0.06 | 78.00 | 74.44 |

2195 Al-Li, $F_{tu} = 78$ ksi, $F_{ty} = 77$ ksi, $\epsilon_{psult} = 0.06$

| Far-Field Stress (ksi) | Max Strain at Hole | Max Stress at Hole (ksi) | Net Section Stress (ksi) |
|------------------------|--------------------|--------------------------|--------------------------|
| 25.7 | 0.007 | 77.00 | 28.56 |
| 45 | 0.0176 | 77.23 | 50.00 |
| 50 | 0.0221 | 77.35 | 55.56 |
| 55 | 0.0263 | 77.46 | 61.11 |
| 60 | 0.0335 | 77.60 | 66.67 |
| 65 | 0.0509 | 77.83 | 72.22 |
| 67 | 0.06 | 78.00 | 74.44 |

2195 Al-Li, $F_{tu} = 80$ ksi, $F_{ty} = 79$ ksi, $\epsilon_{psult} = 0.06$

| Far-Field Stress (ksi) | Max Strain at Hole | Max Stress at Hole (ksi) | Net Section Stress (ksi) |
|------------------------|--------------------|--------------------------|--------------------------|
| 25.7 | 0.007182 | 79.00 | 28.56 |
| 45 | 0.0172 | 79.14 | 50.00 |
| 50 | 0.0216 | 79.20 | 55.56 |
| 55 | 0.0258 | 79.26 | 61.11 |
| 60 | 0.0312 | 79.33 | 66.67 |
| 65 | 0.0457 | 79.53 | 72.22 |
| 69 | 0.06 | 80.00 | 76.67 |

Table 2. Hole stresses and strains versus far-field stress for various 2195 Al-Li materials.

SLWT ET Stress Concentration Analyses, 3.75-in Wide Plates With Holes

2195 Al-Li, $F_{tu} = 78$ ksi, $F_{ty} = 77$ ksi, $\epsilon_{psult} = 0.08$

| Far-Field Stress (ksi) | Max Strain at Hole | Max Stress at Hole (ksi) | Net Section Stress (ksi) |
|------------------------|--------------------|--------------------------|--------------------------|
| 25.7 | 0.007 | 77.00 | 28.56 |
| 45 | 0.0176 | 77.14 | 50.00 |
| 50 | 0.022 | 77.21 | 55.56 |
| 55 | 0.0264 | 77.27 | 61.11 |
| 60 | 0.0322 | 77.34 | 66.67 |
| 65 | 0.0508 | 77.60 | 72.22 |
| 70 | 0.081 | 78.00 | 77.78 |

2195 Al-Li, $F_{tu} = 78$ ksi, $F_{ty} = 73$ ksi, $\epsilon_{psult} = 0.04$

| Far-Field Stress (ksi) | Max Strain at Hole | Max Stress at Hole (ksi) | Net Section Stress (ksi) |
|------------------------|--------------------|--------------------------|--------------------------|
| 24.3 | 0.006636 | 73.00 | 27.00 |
| 45 | 0.0184 | 74.75 | 50.00 |
| 50 | 0.0223 | 75.35 | 55.56 |
| 55 | 0.0277 | 76.16 | 61.11 |
| 60 | 0.0393 | 77.90 | 66.67 |

2195 Al-Li, $F_{tu} = 82$ ksi, $F_{ty} = 77$ ksi, $\epsilon_{psult} = 0.04$

| Far-Field Stress (ksi) | Max Strain at Hole | Max Stress at Hole (ksi) | Net Section Stress (ksi) |
|------------------------|--------------------|--------------------------|--------------------------|
| 25.7 | 0.007 | 77.00 | 28.56 |
| 45 | 0.0173 | 78.59 | 50.00 |
| 50 | 0.0213 | 79.20 | 55.56 |
| 55 | 0.0257 | 79.86 | 61.11 |
| 60 | 0.0347 | 81.21 | 66.67 |
| 65 | 0.0427 | 82.00 | 72.22 |

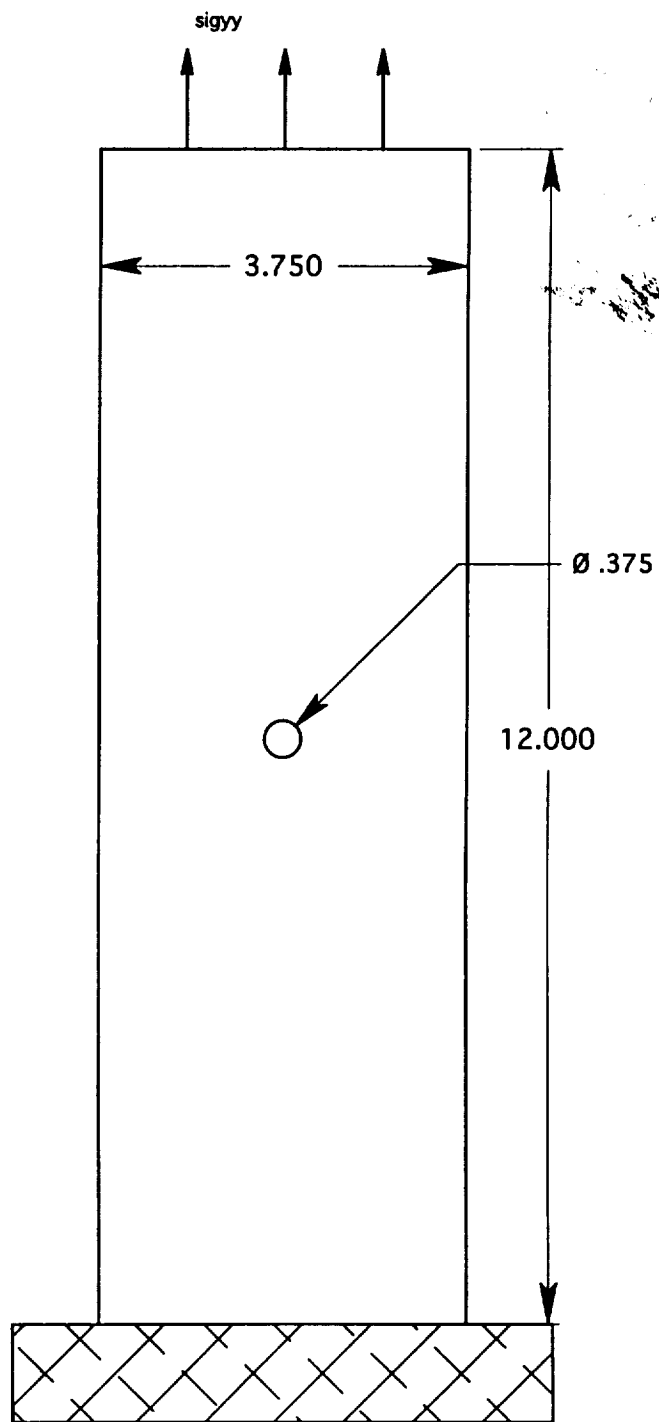


Figure 1. Geometry used in plate with hole analysis.

ORIGINAL PAGE IS
OF POOR QUALITY

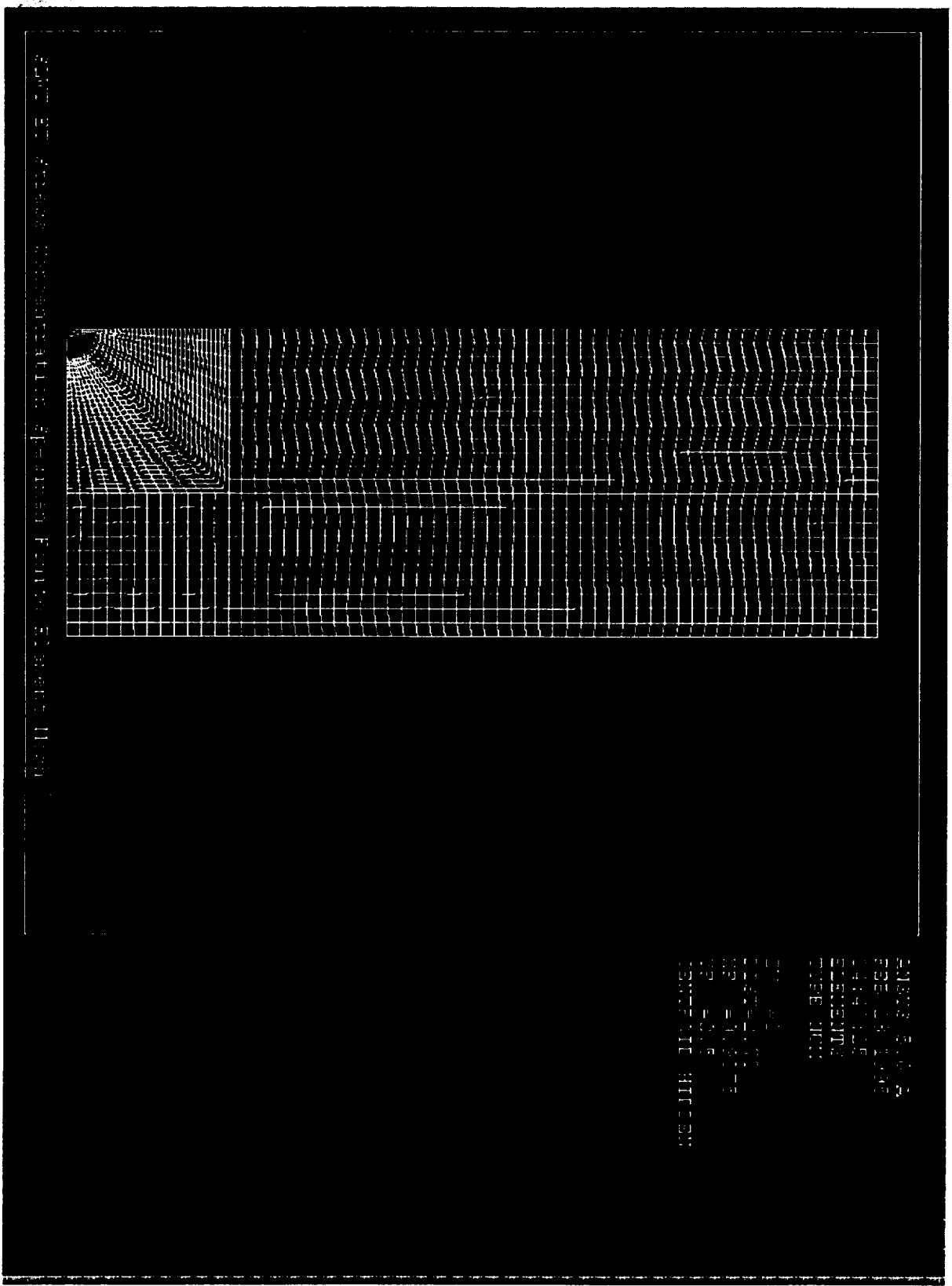


Figure 2. MSFC ANSYS model used in plate with hole analysis.

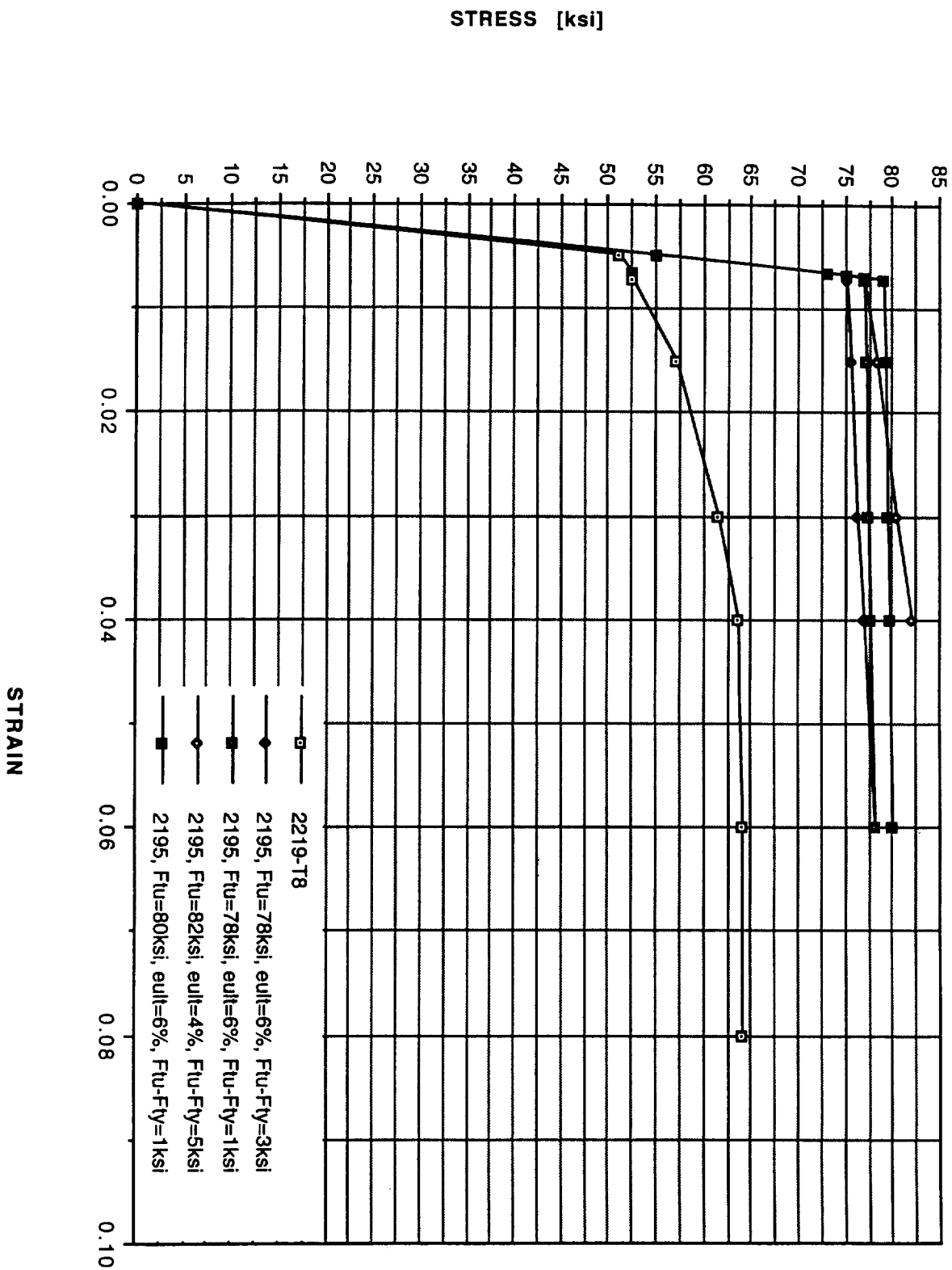


Figure 3. 2195 Al-Li and 2219 Al stress-strain curves.

8.

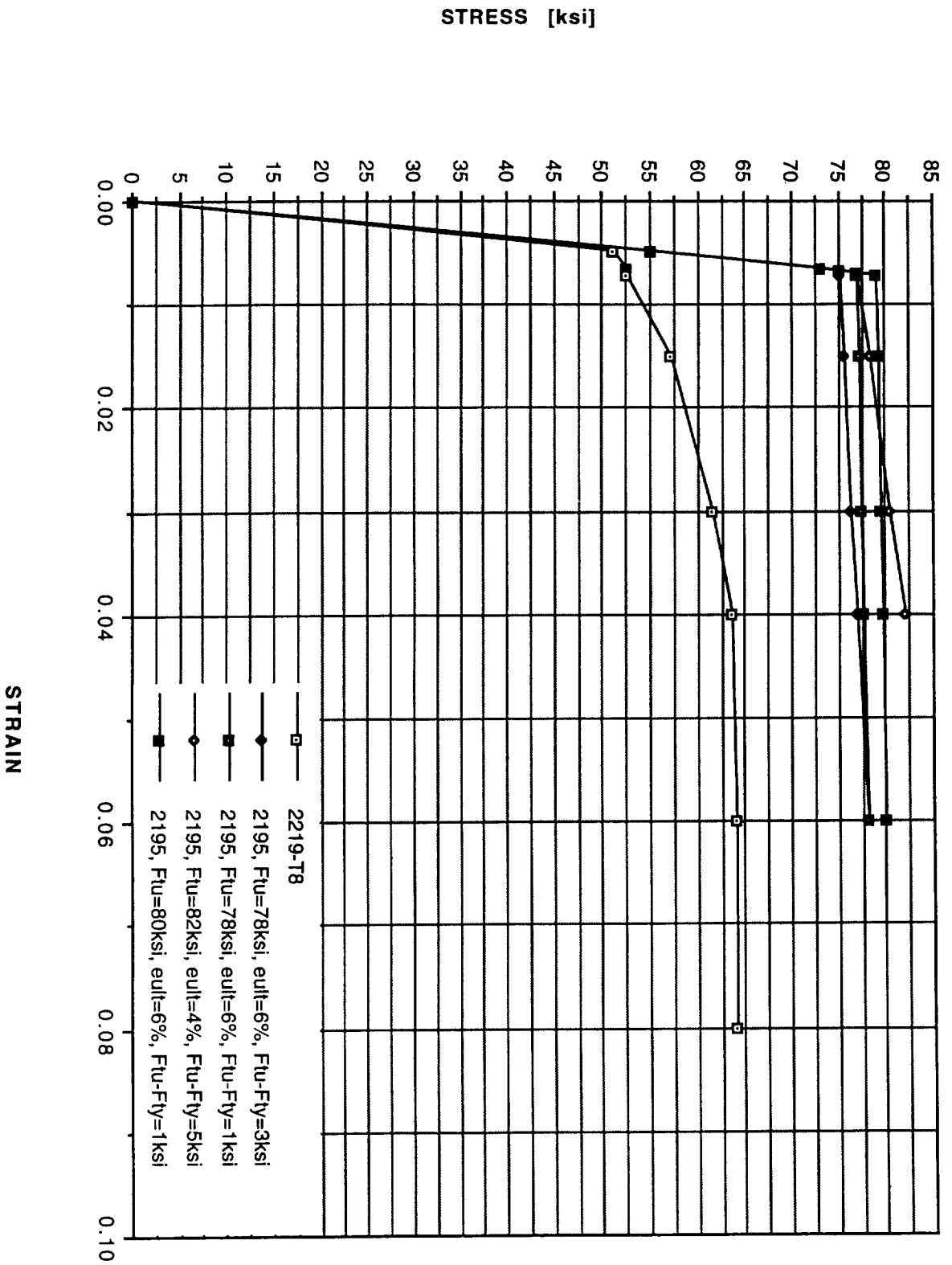
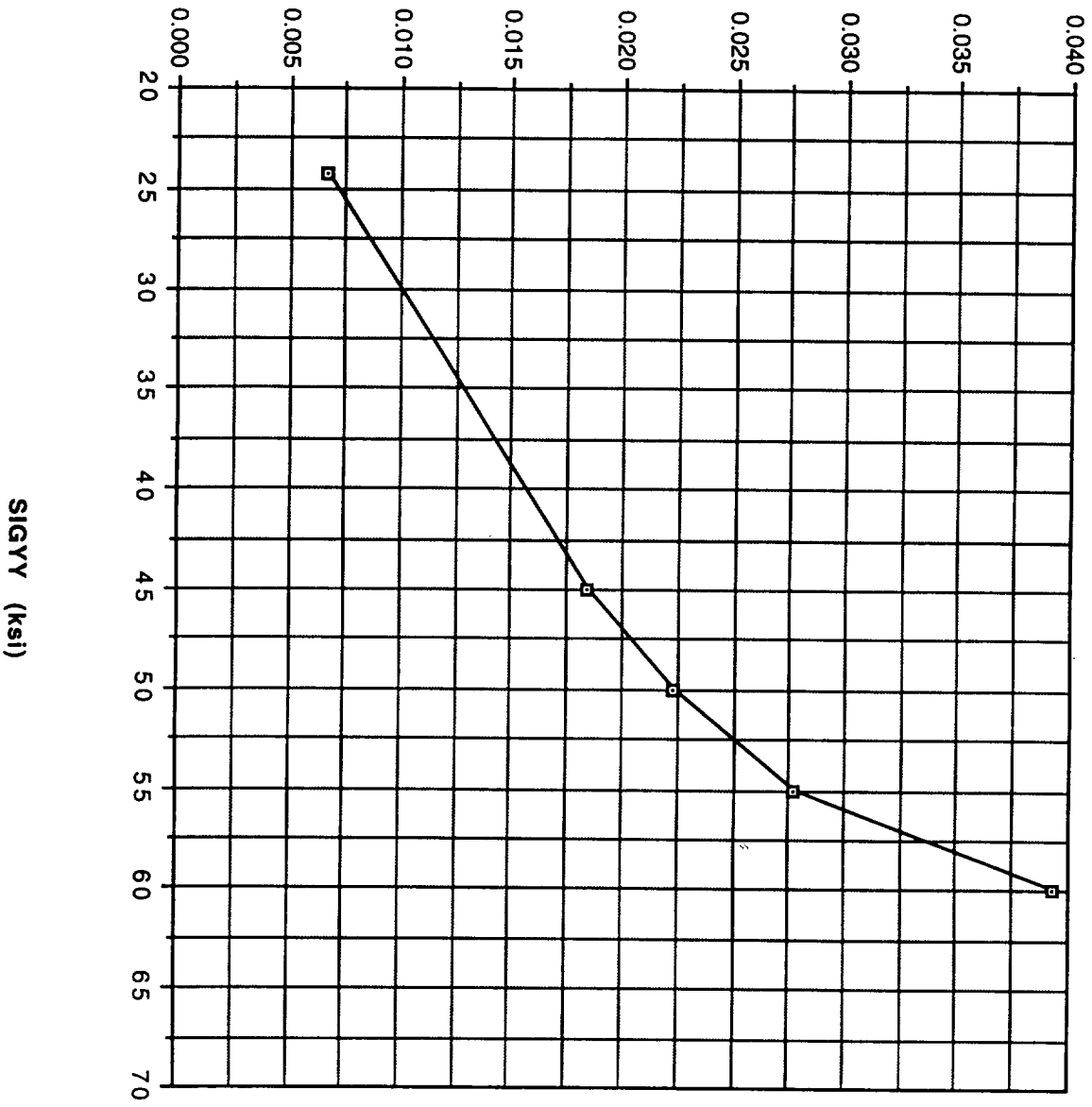


Figure 4. 2195 Al-Li and 2219 Al stress-strain curves.

10

MAX HOLE STRAIN



—□— MAX HOLE STRAIN

10.

Figure 5. Maximum hole strain versus far-field stress, 2195 Al-Li, $F_{tu} = 78$ ksi, $F_{ty} = 73$ ksi, ultimate strain = 0.04.

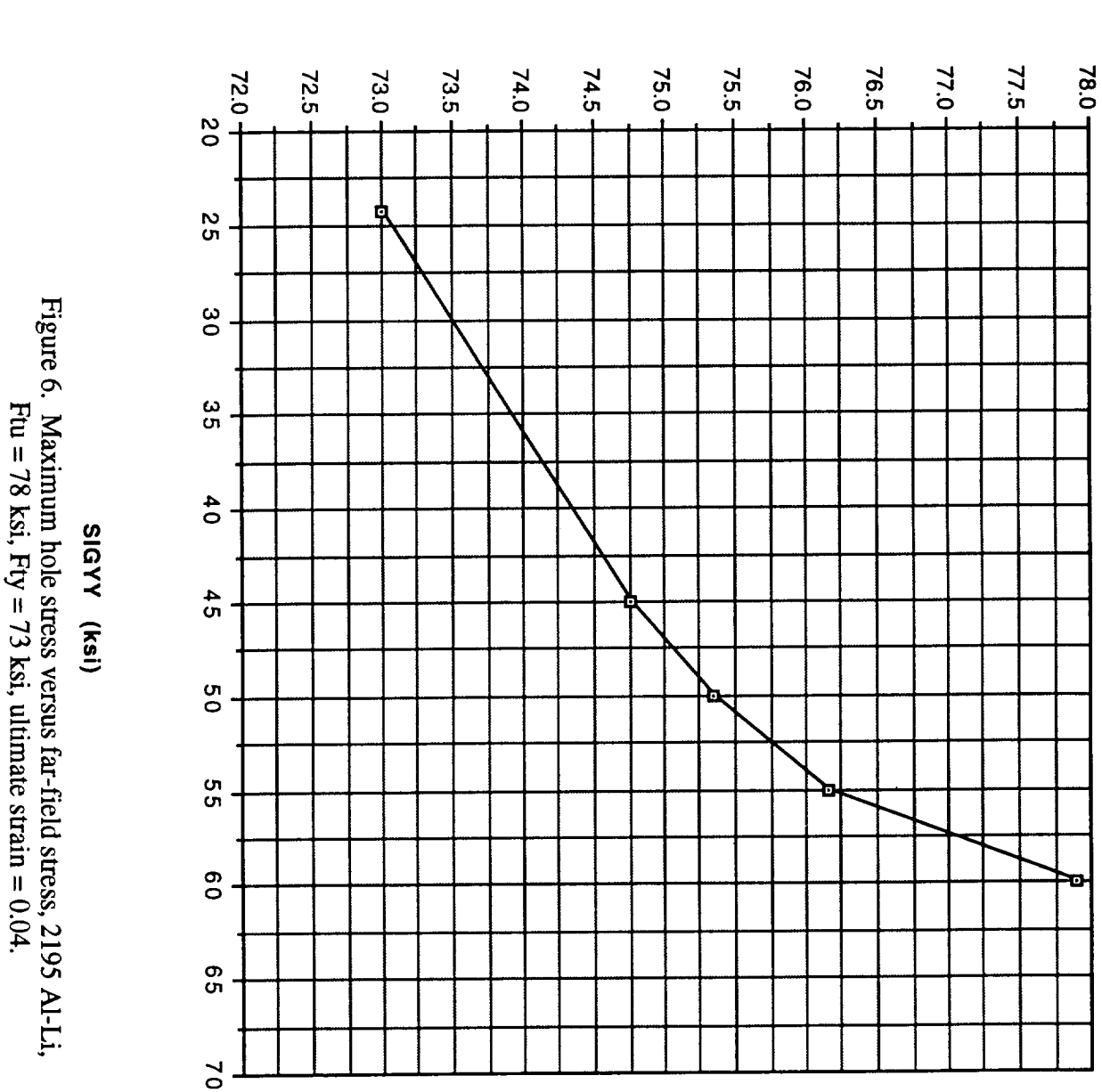


Figure 6. Maximum hole stress versus far-field stress, 2195 Al-Li, $F_{tu} = 78$ ksi, $F_{ty} = 73$ ksi, ultimate strain = 0.04.

MAX HOLE STRESS (ksi)

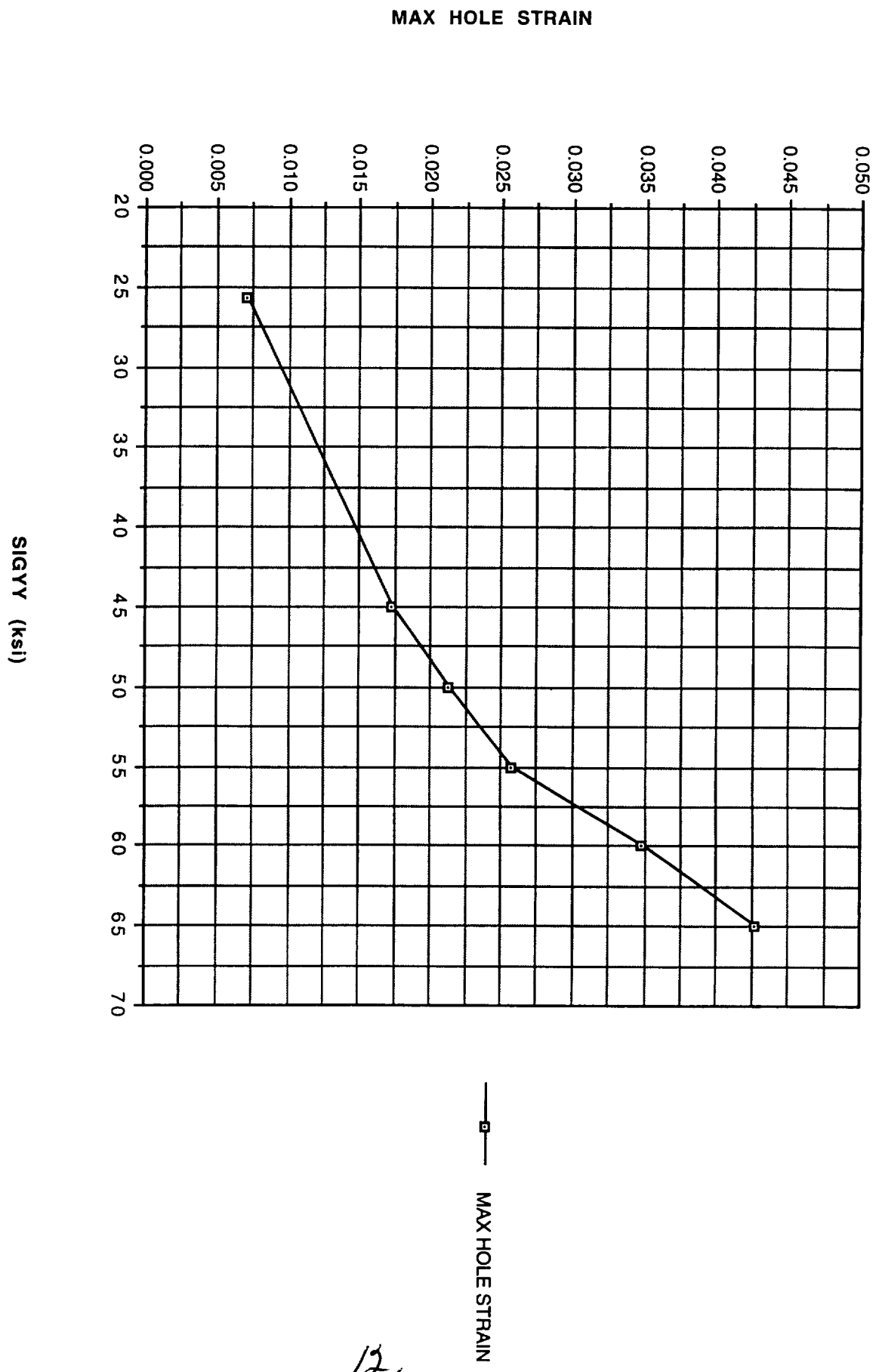


Figure 7. Maximum hole strain versus far-field stress, 2195 Al-Li, $F_{tu} = 82$ ksi, $F_{ty} = 77$ ksi, ultimate strain = 0.04.

MAX HOLE STRESS (ksi)

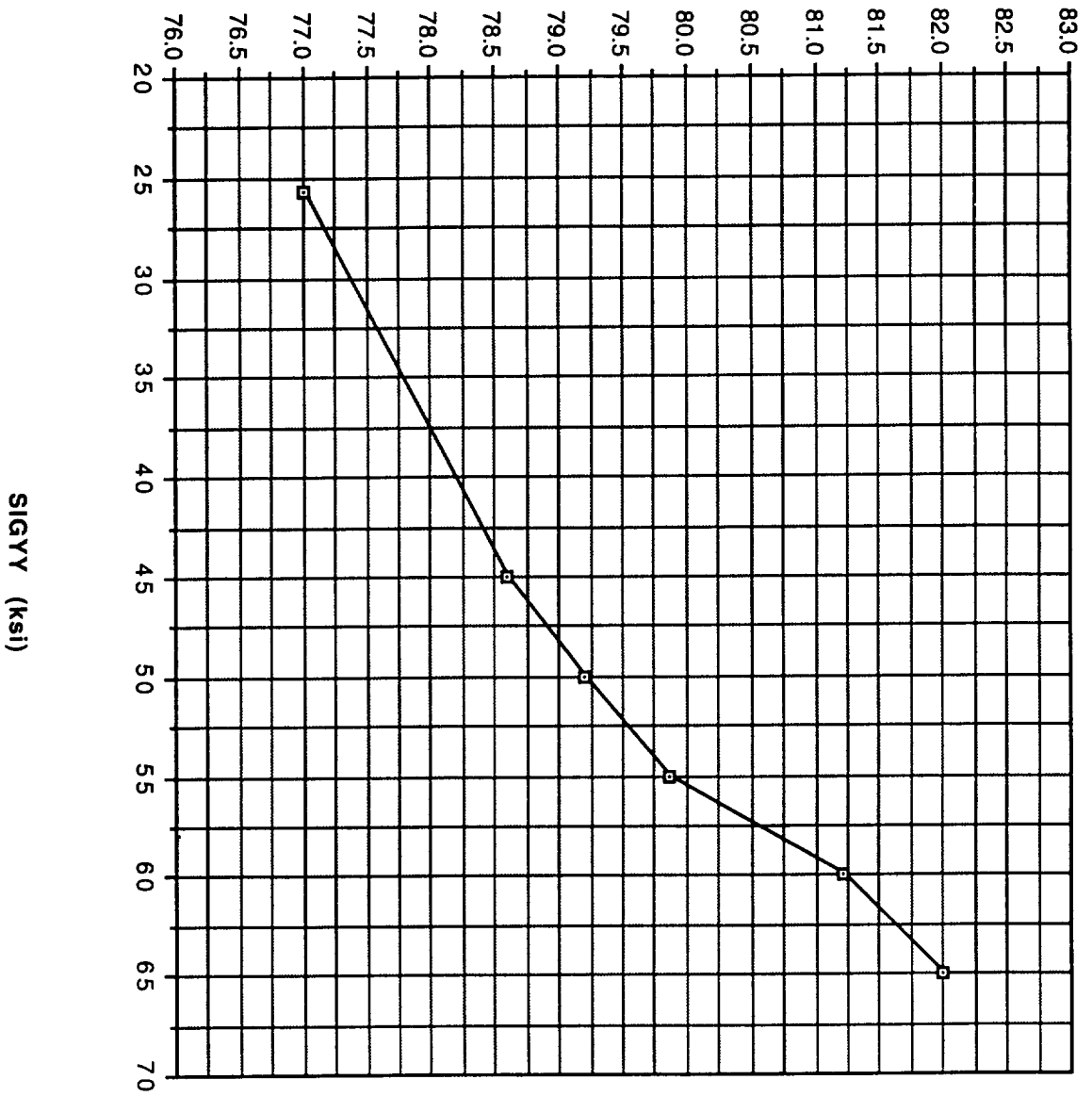


Figure 8. Maximum hole stress versus far-field stress, 2195 Al-Li, $F_{tu} = 82$ ksi, $F_{ty} = 77$ ksi, ultimate strain = 0.04.

—□— MAX HOLE STRESS (ksi)

~~3~~

14

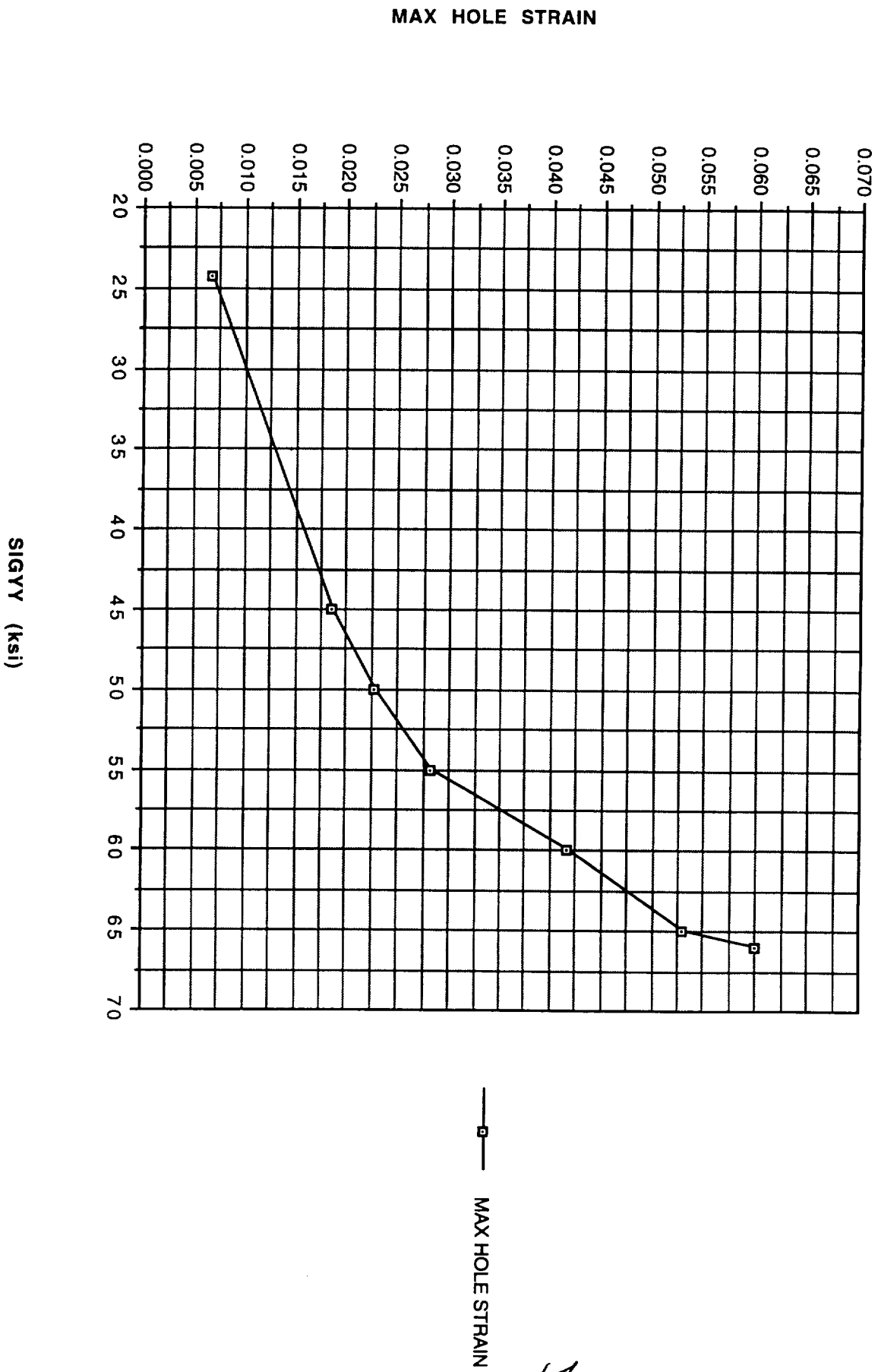


Figure 9. Maximum hole strain versus far-field stress, 2195 Al-Li, $F_{tu} = 78$ ksi, $F_{ty} = 73$ ksi, ultimate strain = 0.06.

14

MAX HOLE STRESS (ksi)

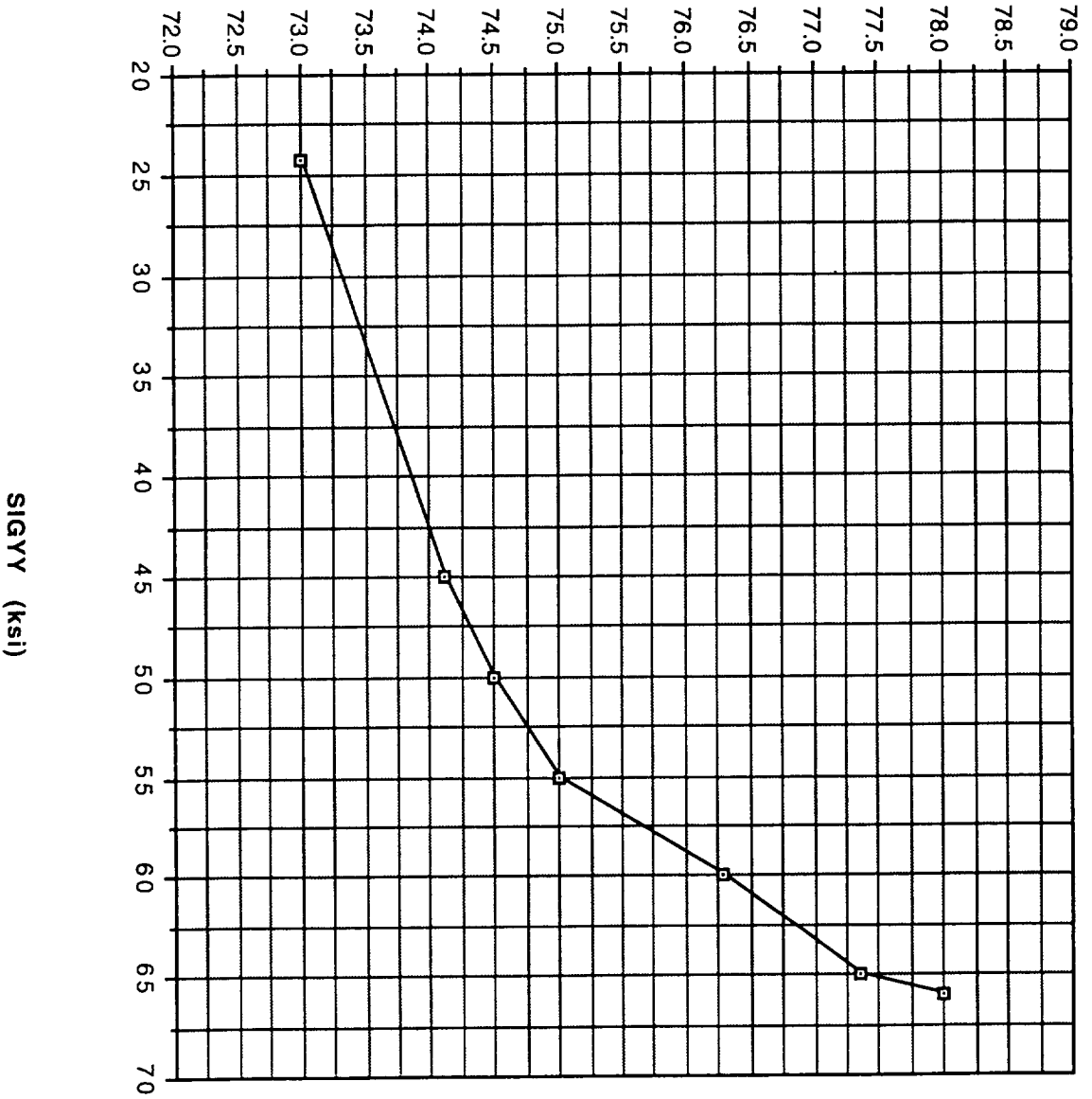


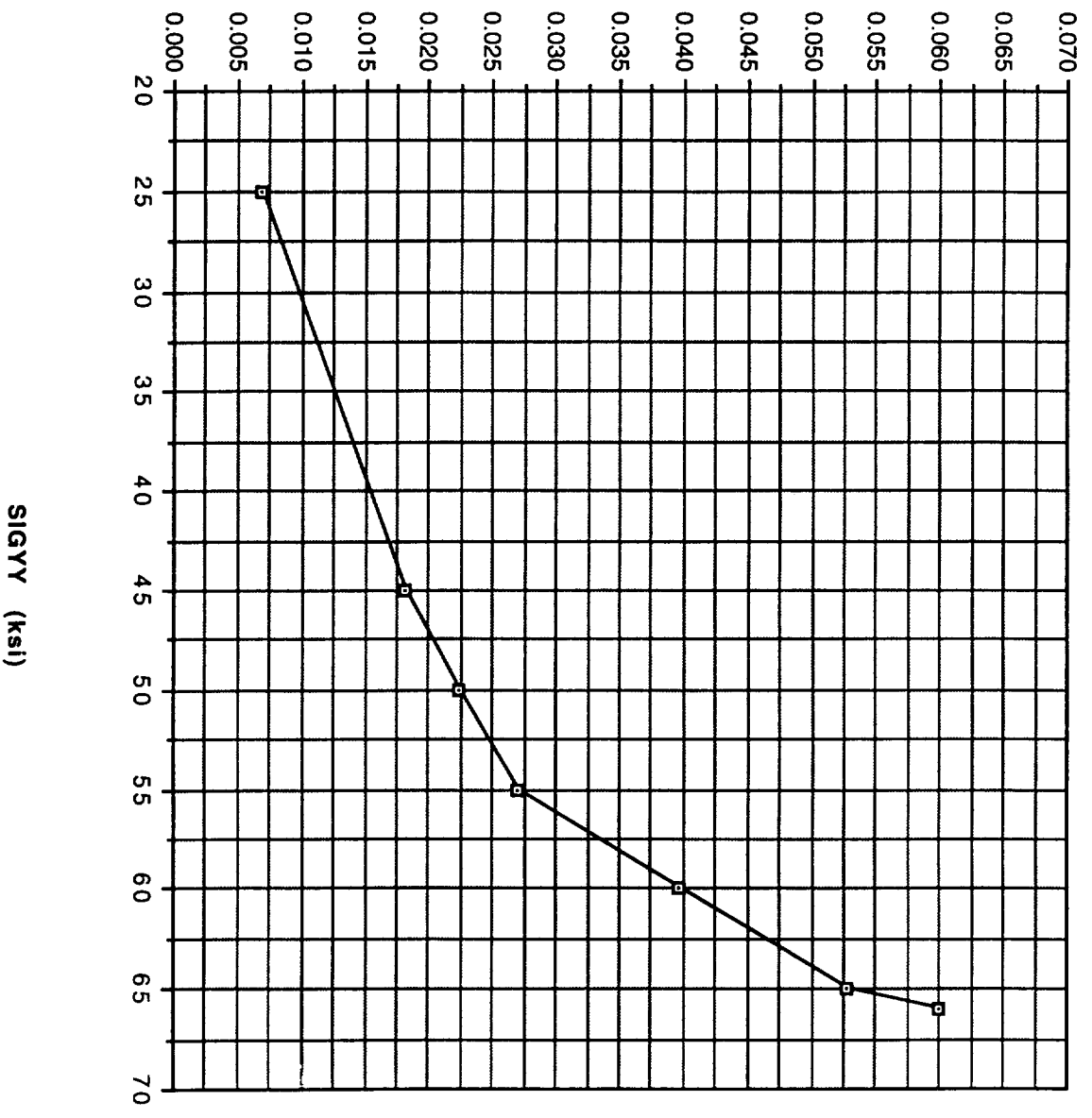
Figure 10. Maximum hole stress versus far-field stress, 2195 Al-Li,
F_{tu} = 78 ksi, F_{ty} = 73 ksi, ultimate strain = 0.06.

—□— MAX HOLE STRESS (ksi)

15.

7

MAX HOLE STRAIN



—□— MAX HOLE STRAIN

Figure 11. Maximum hole strain versus far-field stress, 2195 Al-Li, $F_{tu} = 78$ ksi, $F_{ty} = 75$ ksi, ultimate strain = 0.06.

17

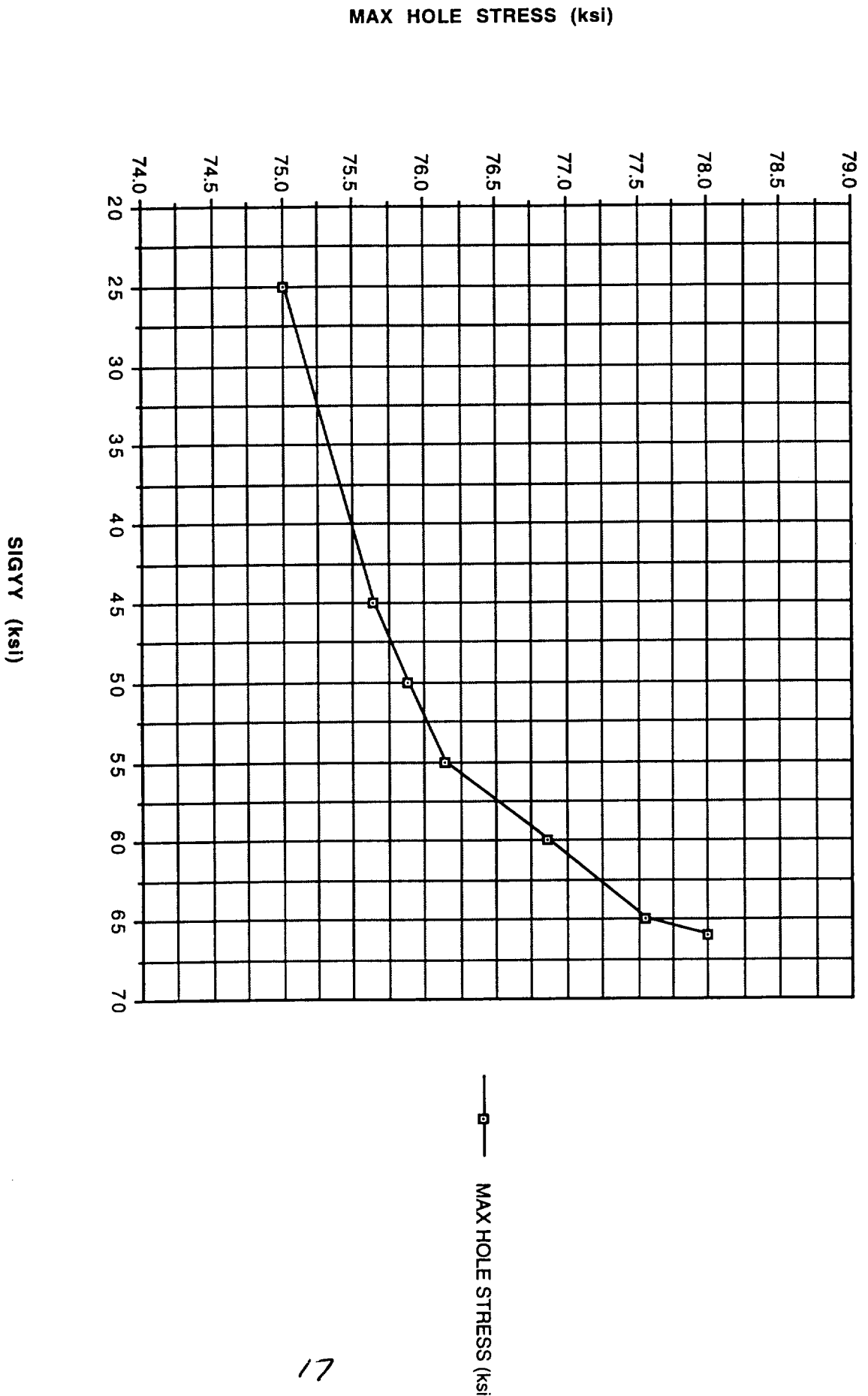


Figure 12. Maximum hole stress versus far-field stress, 2195 Al-Li, $F_{tu} = 78$ ksi, $F_{ty} = 75$ ksi, ultimate strain = 0.06.

17

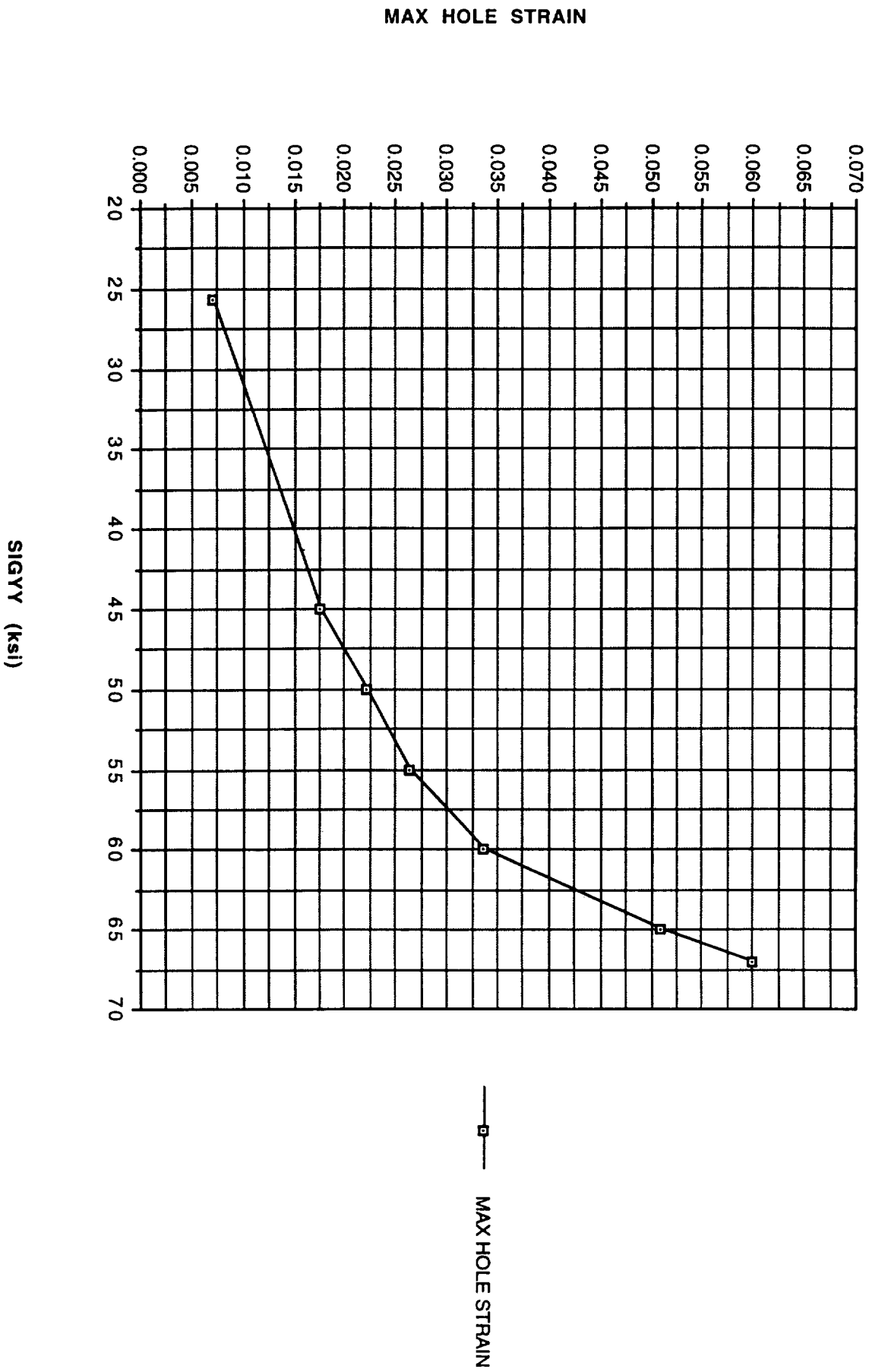
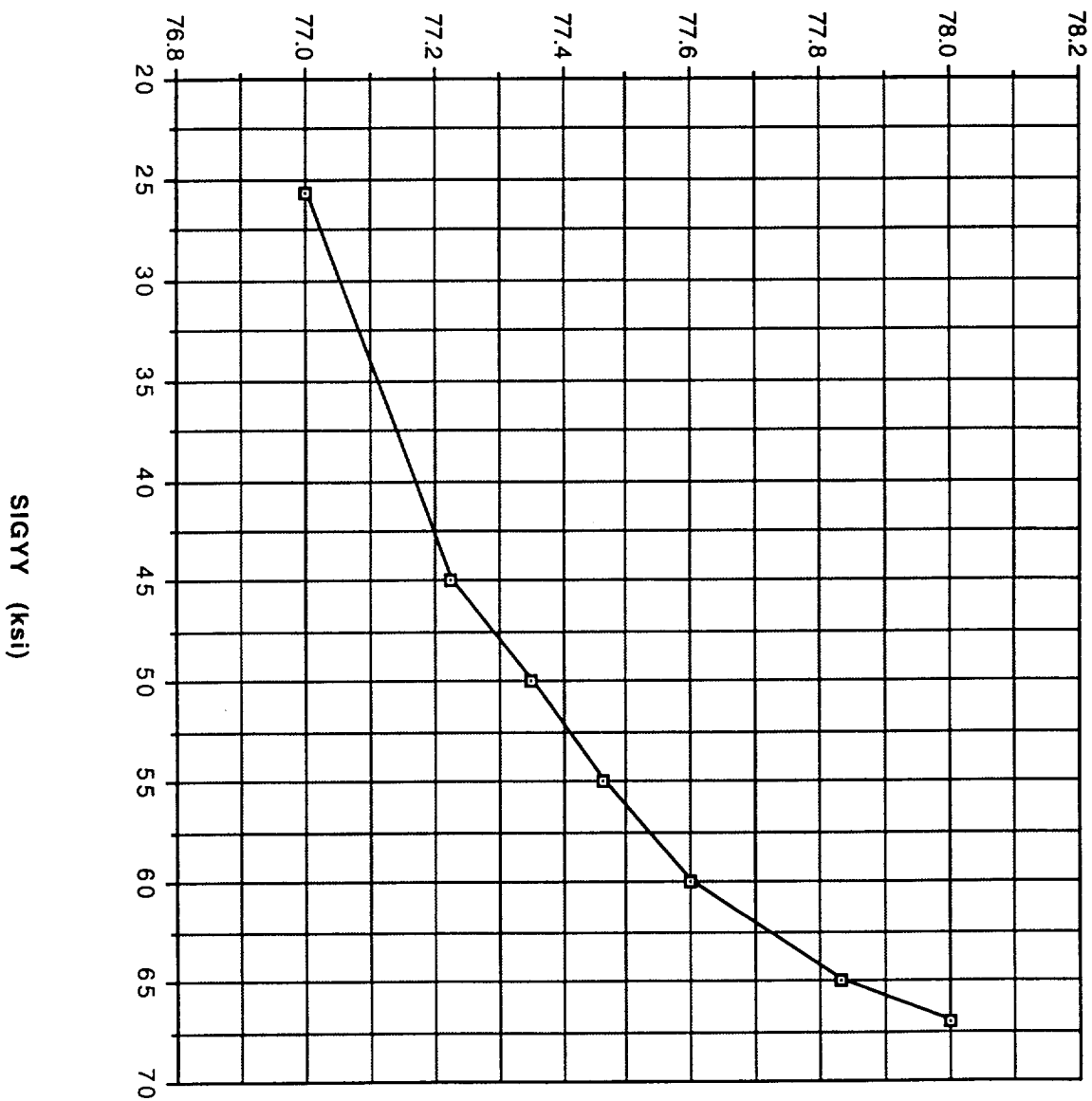


Figure 13. Maximum hole strain versus far-field stress, 2195 Al-Li, $F_{tu} = 78$ ksi, $F_{ty} = 77$ ksi, ultimate strain = 0.06.

MAX HOLE STRESS (ksi)



—□— MAX HOLE STRESS (ksi)

Figure 14. Maximum hole stress versus far-field stress, 2195 Al-Li, $F_{tu} = 78$ ksi, $F_{ty} = 77$ ksi, ultimate strain = 0.06.

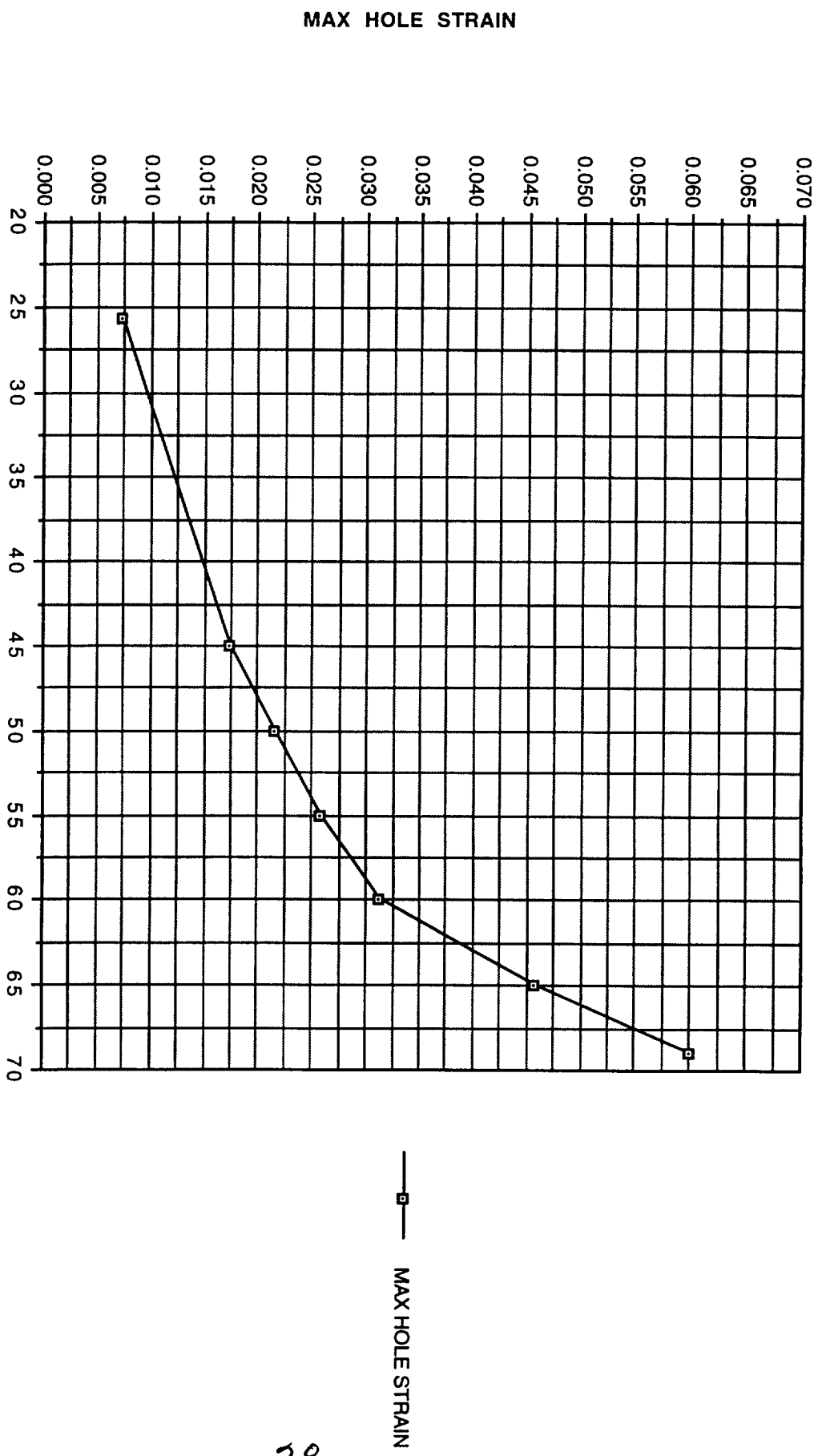


Figure 15. Maximum hole strain versus far-field stress, 2195 Al-Li, $F_{tu} = 80$ ksi, $F_{ty} = 79$ ksi, ultimate strain = 0.06.

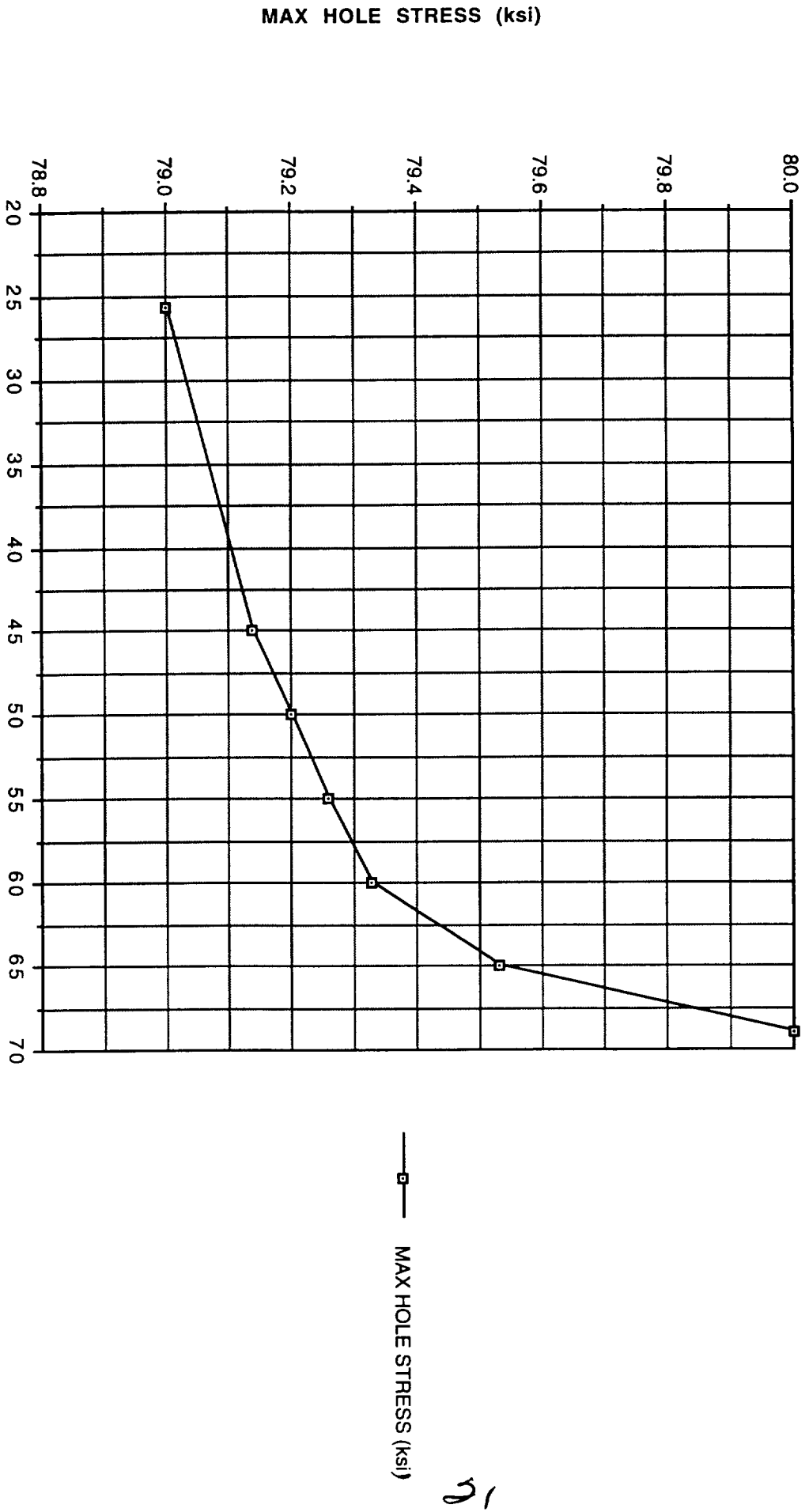


Figure 16. Maximum hole stress versus far-field stress, 2195 Al-Li, $F_{tu} = 80$ ksi, $F_{ty} = 79$ ksi, ultimate strain = 0.06.

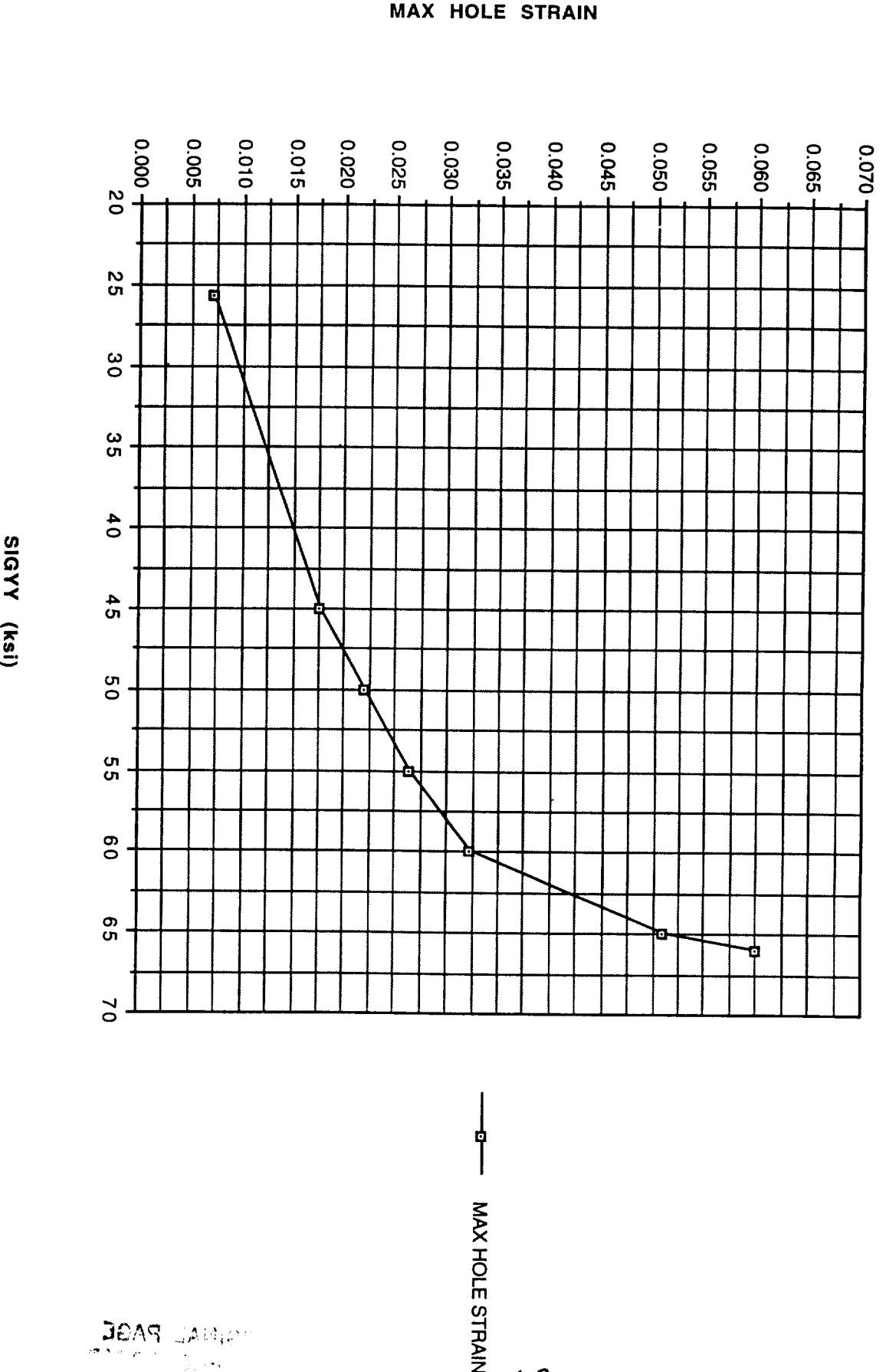
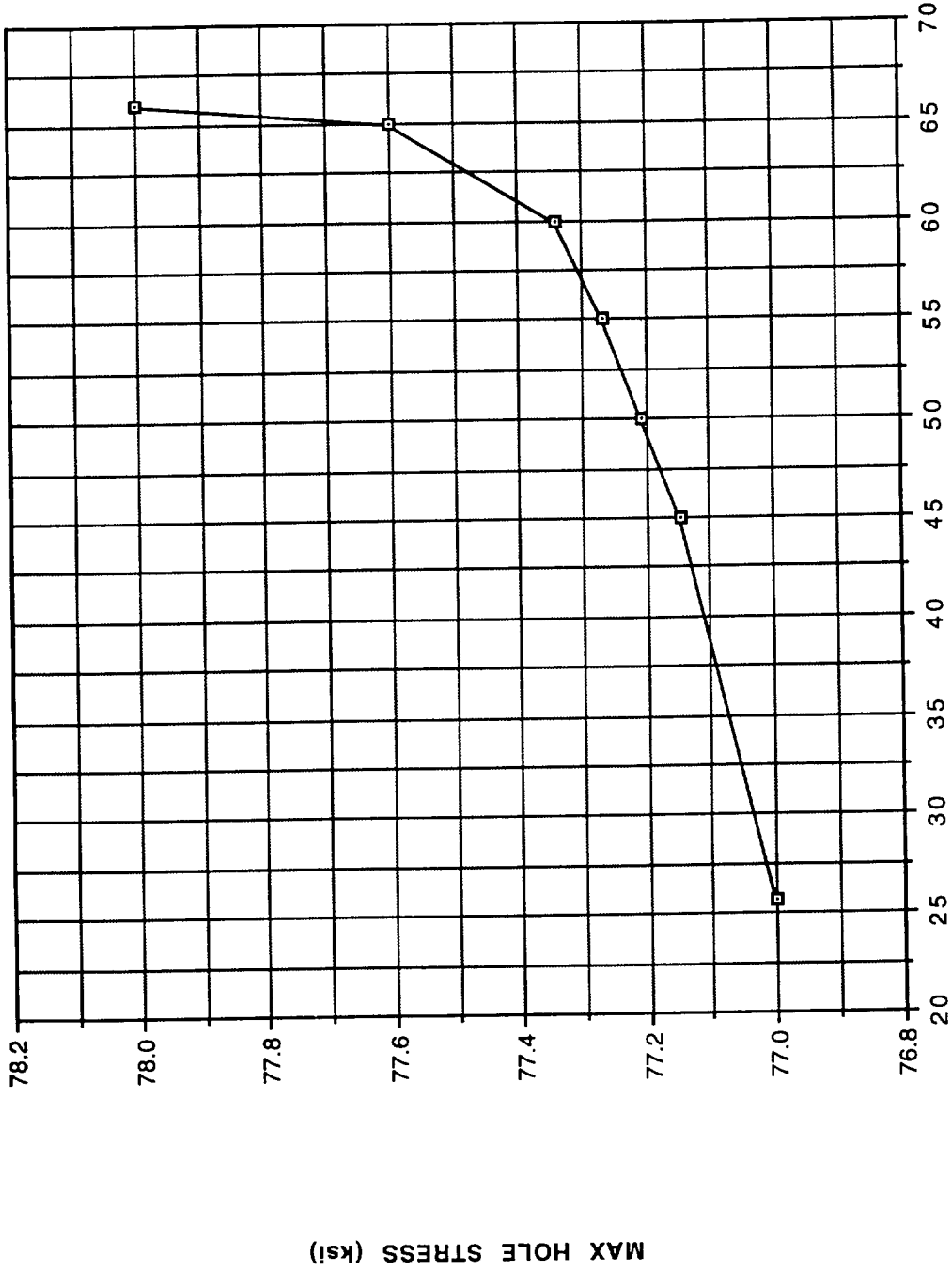


Figure 17. Maximum hole strain versus far-field stress, 2195 Al-Li, $F_{tu} = 78$ ksi, $F_{ty} = 77$ ksi, ultimate strain = 0.08.

—□— MAX HOLE STRAIN

REVISIONS
PAGE 1



MAX HOLE STRESS (ksi)



23

SIGY (ksi)

Figure 18. Maximum hole stress versus far-field stress, 2195 Al-Li, $F_{tu} = 78$ ksi, $F_{ty} = 77$ ksi, ultimate strain = 0.08.

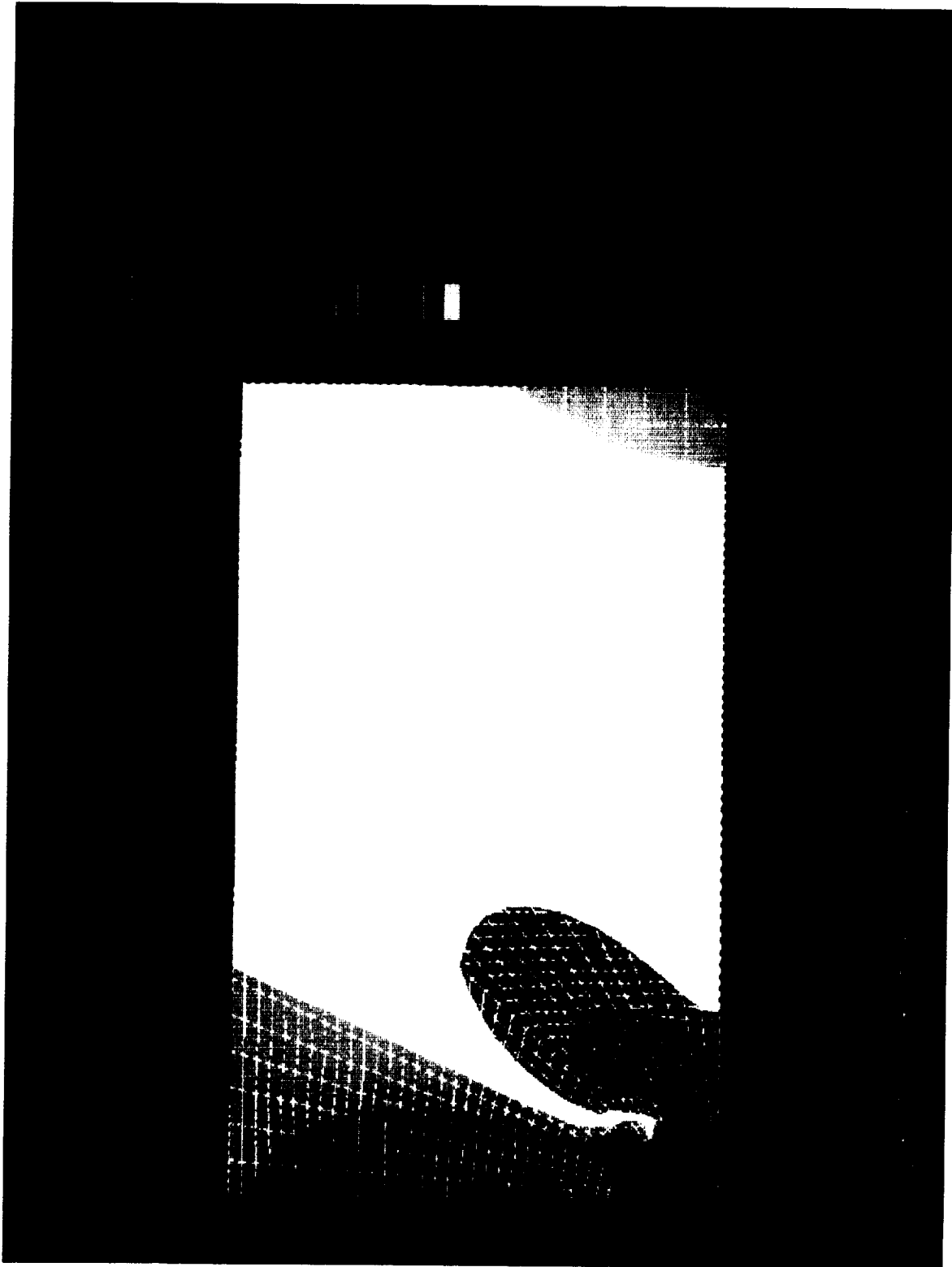


Figure 19. Plot of von Mises stress for 2195 plate with hole, $F_{tu} = 78$ ksi, $F_{ty} = 73$ ksi, ultimate strain = 4 percent, far-field stress = 60 ksi.

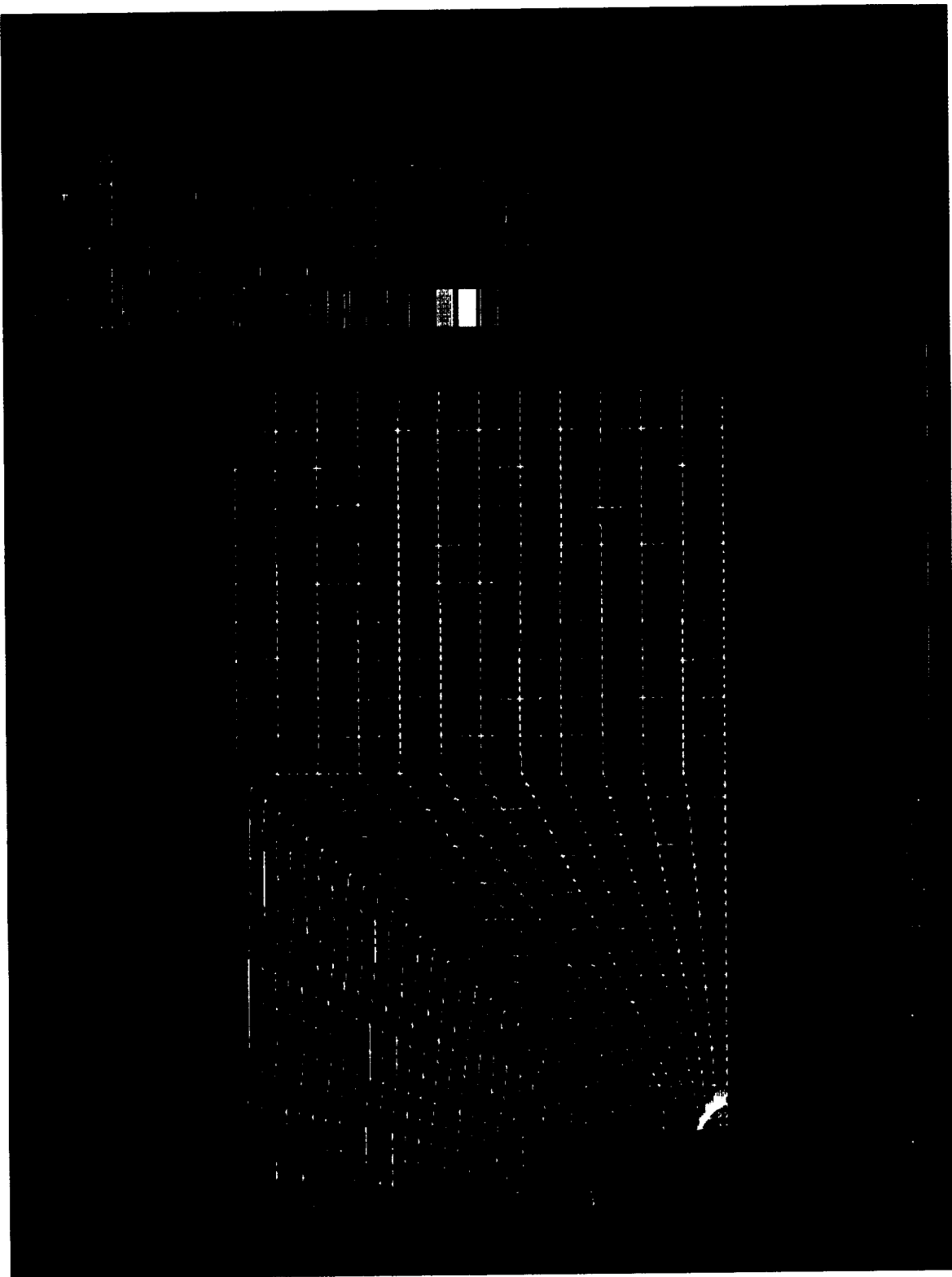


Figure 20. Plot of axial strain for 2195 plate with hole, $F_{tu} = 789$ ksi, $F_{ty} = 73$ ksi, ultimate strain = 4 percent, far-field stress = 60 ksi.

ORIGINAL PAGE
COLOR PHOTOGRAPH

REFERENCES

1. ANSYS, Inc. (formerly Swanson Analysis Systems, Inc.): "ANSYS User's Manual (Revision 5.0)." December 1992.
2. Timoshenko, S.P., and Goodier, J.N.: "Theory of Elasticity." McGraw-Hill, 1970.
3. Malvern, L.E.: "Introduction to the Mechanics of a Continuous Medium." Prentice-Hall, 1969.

REPORT DOCUMENTATION PAGEForm Approved
OMB No. 0704-0188

Public reporting burden for this collection of information is estimated to average 1 hour per response, including the time for reviewing instructions, searching existing data sources, gathering and maintaining the data needed, and completing and reviewing the collection of information. Send comments regarding this burden estimate or any other aspect of this collection of information, including suggestions for reducing this burden, to Washington Headquarters Services, Directorate for Information Operations and Reports, 1215 Jefferson Davis Highway, Suite 1204, Arlington, VA 22202-4302, and to the Office of Management and Budget, Paperwork Reduction Project (0704-0188), Washington, DC 20503.

| | | | | |
|---|---|--|---|--|
| 1. AGENCY USE ONLY (Leave blank) | | 2. REPORT DATE May 1995 | 3. REPORT TYPE AND DATES COVERED Technical Paper | |
| 4. TITLE AND SUBTITLE Analysis of Stress Concentration at Holes in Components Made of 2195 Aluminum-Lithium | | | 5. FUNDING NUMBERS | |
| 6. AUTHOR(S) R. Ahmed | | | | |
| 7. PERFORMING ORGANIZATION NAME(S) AND ADDRESS(ES) George C. Marshall Space Flight Center Marshall Space Flight Center, Alabama 35812 | | | 8. PERFORMING ORGANIZATION REPORT NUMBER M-781 | |
| 9. SPONSORING / MONITORING AGENCY NAME(S) AND ADDRESS(ES) National Aeronautics and Space Administration Washington, DC 20546-0001 | | | 10. SPONSORING / MONITORING AGENCY REPORT NUMBER NASA TP-3554 | |
| 11. SUPPLEMENTARY NOTES Prepared by Structures and Dynamics Laboratory, Science and Engineering Directorate. | | | | |
| 12a. DISTRIBUTION / AVAILABILITY STATEMENT Unclassified-Unlimited Subject Category 39 | | | 12b. DISTRIBUTION CODE | |
| 13. ABSTRACT (Maximum 200 words) Because the 2195 aluminum-lithium of the super lightweight external tank (SLWT ET) has a lower toughness than the 2219 aluminum used in previous ET's, careful attention must be paid to stress concentration in the SLWT ET. This report details the initial analysis performed by NASA to determine the material properties required to ensure structural integrity in these critical areas. | | | | |
| 14. SUBJECT TERMS external tank, liquid hydrogen tank, stress concentration, plasticity, nonlinear analysis, aluminum-lithium | | | 15. NUMBER OF PAGES 32 | |
| | | | 16. PRICE CODE A03 | |
| 17. SECURITY CLASSIFICATION OF REPORT Unclassified | 18. SECURITY CLASSIFICATION OF THIS PAGE Unclassified | 19. SECURITY CLASSIFICATION OF ABSTRACT Unclassified | 20. LIMITATION OF ABSTRACT Unlimited | |

